DOI 10.1007/s10527-020-09936-y
Biomedical Engineering, Vol. 53, No. 5, January, 2020, pp. 327-331. Translated from Meditsinskaya Tekhnika, Vol. 53, No. 5, Sep.-Oct., 2019, pp. 22-25. Original article submitted September 21, 2018.

Use of Inverse Emulsions Based on Siloxanes to Monitor Apparent Diffusion Coefficients in Magnetic Resonance Tomography

K. A. Sergunova

A method for evaluating and standardizing quantitative data for diffusion-weighted (DW) magnetic resonance tomography using a phantom containing an inverse emulsion based on siloxanes is presented. The following characteristics of colloidal systems are addressed: micelle size, chemical phase shifts, proton density, relaxation time, stability, signal intensity on DW images, and the apparent diffusion coefficient (ADC). The use of inverse emulsions based on siloxanes provides for measurement not only of the self-diffusion coefficient, but also restricted diffusion, in the same measurement. The accuracy of measurements of ADC using the samples selected for these studies was assessed by statistical analysis of the distribution of signal intensity and computation of the coefficient of variation.

Introduction

Magnetic resonance tomography (magnetic resonance imaging, MRI) is now justifiably regarded as one of the most informative contemporary diagnostic methods, providing not only qualitative assessments of the pathological state of various organs and body systems, but also determining the functional characteristics and metabolism of living tissues using quantitative indicators. For example, diffusion-weighted (DW) MRI can be used to determine apparent diffusion coefficients (ADC), reflecting the mobility of water molecules in tissues. As demonstrated by numerous studies, achievement of particular ADC values can provide serious grounds for suspecting that a space-occupying lesion is malignant or detecting the acquisition of malignancy [1-3].

Nonetheless, there can be differences in measured ADC values not only between instruments from different manufacturers, but between MR tomographs of the same model as well [4]. The accuracy of ADC measurements depends on a good calibration gradient, accurate delivery of gradient impulses and impulse shape, the technical characteristics of the radio-frequency unit, the postprocessing algorithms used, etc. [5]. Incorrect operation of MRI units can lead to the occurrence of systematic measurement errors, which in turn make it impossible to use ADC to assess the degree of malignancy of neoplastic processes or to compare data obtained using different instruments. The effects of systematic errors can be excluded or at least decreased by eliminating the sources of error or by determining correction coefficients.

The importance of identifying systematic errors determines the need to develop appropriate specialized monitoring systems (phantoms) to assess the accuracy of ADC measurements [6, 7].

Scientific and Applied Center for Medical Radiology, Moscow City Health Department, Moscow, Russia; E-mail: sergunova@rpcmr.org.ru

Materials and Methods

The lower limit of the range of ADC was modeled in the previous study [5] using the Einstein–Smoluchowksi equation:

$$D = \frac{kT}{3\pi\eta d}, \quad (1)$$

where d is molecular diameter, k is Boltzmann's constant, η is viscosity coefficient, and T is absolute temperature. Substances with coefficients of viscosity and molecular sizes much greater than those of water were considered in [5]: agarose, agar agar, polyacrylamide, low molecular weight silicone rubber, polydimethylsiloxane, etc.

However, signal intensity on DW images is determined not only by the rate of diffusion, but also by the spin–spin relaxation time T_2:

$$I_{DWI} = k_H \left(1 - e^{-\frac{TR}{T_1}}\right) e^{-\frac{TE}{T_2}} e^{-b \cdot \mathrm{ADC}}, \quad (2)$$

where TR is the time interval between two radio-frequency (RF) impulses; TE is the time interval between the RF impulse and the peak of the echo signal, and k_H is a coefficient which depends on proton density.

That is why organic silicon compounds with low ADC and high T_2 values were selected for further tests: cyclomethicone [8] and caprylyl methicone, for which computed diffusion coefficients are 0.2 and 0.08 mm^2/s, respectively.

Measurements of times T_1 and T_2 were performed using a Bruker Minispec relaxometer with a working frequency of 60 MHz, which is close to the resonance frequency of 62.4 MHz of hydrogen nuclei in a 1.5-T induction field. Values of T_1 and T_2 for cyclomethicone are 1070 ± 20 and 720 ± 20 ms, respectively, while those for caprylyl are 950 ± 20 and 174 ± 7 ms.

These organic silicon compounds were used as the oil dispersion medium to make emulsions of the water-in-oil type, where micelle formation leads to restricted movement of water molecules, resulting in a decrease in ADC. Preparation of homogeneous physically stable dispersions (emulsification) was performed in three stages: using a colloid mill at 57 ± 3°C and a rate of 10,000-17,000 rpm, then for 30 s at 25,000 rpm, and then with an IKA Ultra Turrax T25 ultrasound disperser.

Colloid stability was determined by centrifugation to establish the percentage content of the phase of interest (oil or water). Dispersion analysis on a Beckman Coulter LS230 was used to compare micelle size distributions in emulsions immediately after emulsification and after 14 days.

The fat suppression function is often used in DW MRI. Therefore, to assess the intensity of signal from emulsions in DW images by MR spectroscopy, the proton density of the dispersion phase (water) and the chemical shifts for fat and water were measured. ^{1}H MR spectra were obtained using a Bruker Tomikon S 50 0.5-T MR scanner (TR = 3000 ms; TE = 17.4 ms; field size, 30 × 20 mm; voxel size, 10 × 10 × 10 mm; averaging number = 16).

The emulsion signal intensity distribution was analyzed and the coefficient of variation was calculated for different values of the b factor in order to determine the accuracy of ADC measurement using the selected samples.

Results

Figure 1 shows ^{1}H MR spectra of pure substances (water and cyclomethicone) and the emulsions prepared from them. Chemical shifts Δ_{ppm} for siloxanes (cyclomethicone and caprylyl) relative to water were ~5.0 ppm (for -CH_3 groups) and ~3.9 ppm (for -CH_2 groups). Δ_{ppm} for hydrogen groups in water molecules in micelles was no greater than 0.25 ppm.

According to Eq. (3), for a bandpass Δf = 16 kHz, the number of pixels n = 128, and pixel size of 5 mm, in

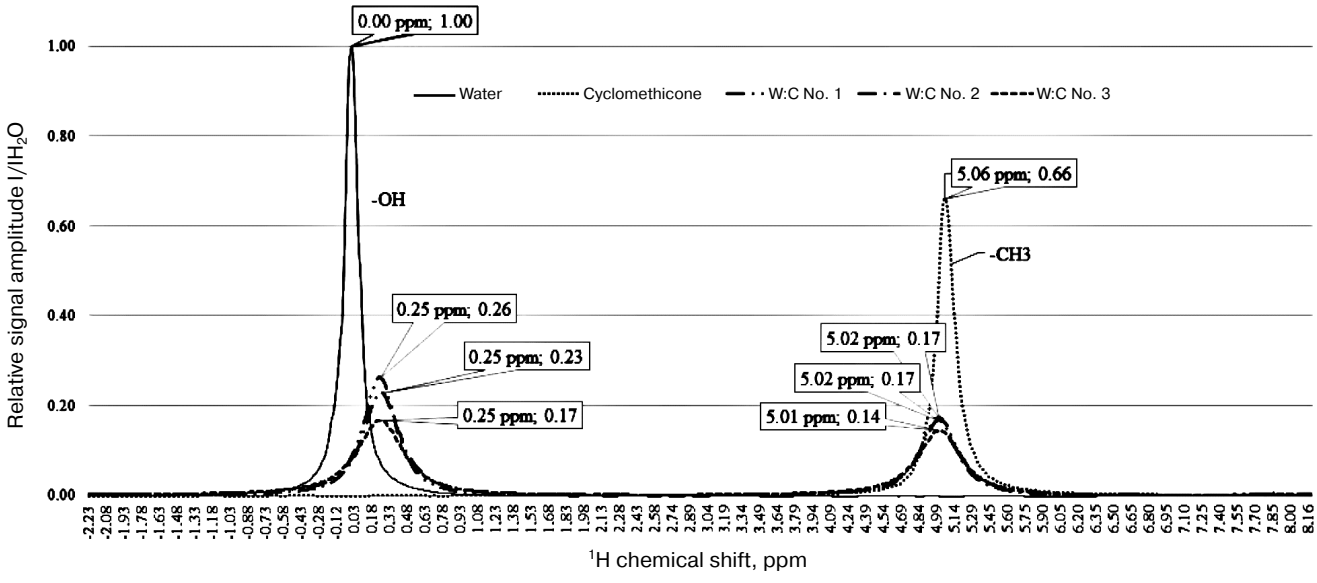

Fig. 1. ^{1}H NMR spectra of pure substances and emulsions based on cyclomethicone.

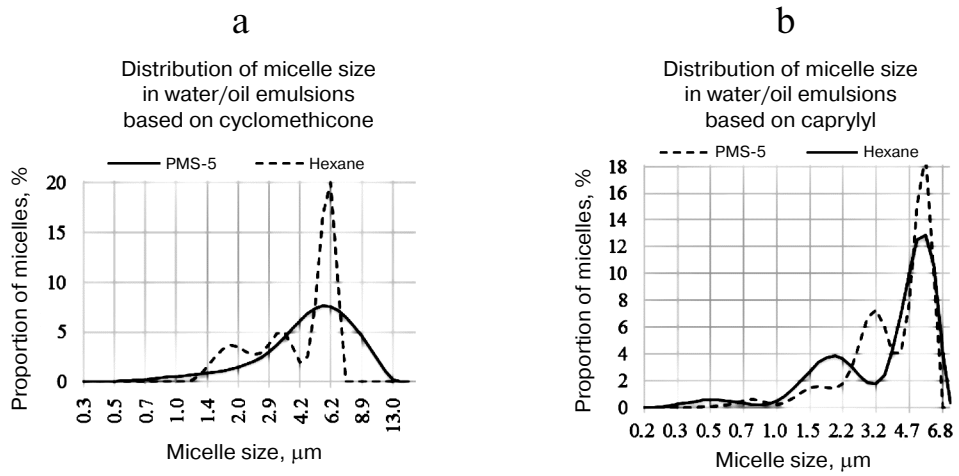

Fig. 2. Distribution of micelle size for inverse emulsions (water/oil): a) based on cyclomethicone (50%) containing 7.4% emulsifier; b) based on caprylyl (50%) containing 7.4% emulsifier.

the direction of frequency coding for an MR tomograph with magnetic induction $B = 1.5$ T, displacements of the emulsion signals l were 0.6 mm for the dispersed phase (the aqueous phase) and 12.8 mm for the dispersion medium (the oil phase):

$$l = \frac{\gamma \cdot B \cdot \Delta_{ppm}}{\Delta f / n}, \quad (3)$$

where γ is the hydromagnetic ratio and Δ_{ppm} is the chemical shift.

This provides for phase separation on DW images and assessment of the accuracy of measurements of ADC for the restricted diffusion of water molecules within micelles D_m and the self-diffusion D_c of siloxane molecules in emulsions [9]. The proposed technical solution is in good agreement with the biexponential model used to describe diffusion in living tissue [10-12]:

$$S_n = f \cdot e^{-b \cdot \mathrm{ADC}_r(\Delta, R)} + (1 - f) \cdot e^{-b \cdot \mathrm{ADC}_o}, \quad (4)$$

where ADC_r is the apparent coefficient of restricted diffusion which depends on Δ (the time between delivery of the two diffusion-coding gradient impulses) and R (molecular radius), ADC_o is the apparent coefficient of obstructed diffusion, and f is the volume proportion of water molecules with restricted diffusion.

The reported sizes of cells in pathological formations, 3-12 μm [12, 13], are consistent with micelle diameter in inverse emulsions based on cyclomethicone (Fig. 2a) and caprylyl (Fig. 2b). Dispersion analysis indicated that micelle size for the first substance was 4.8 ± 1.8 μm when initial samples were diluted in PMS-5 and 4.2 ± 1.6 μm when diluted in hexane. Values for the second substance were 4.0 ± 1.6 and 3.6 ± 1.8 μm, respectively.

The phantom model allows the dependence of ADC on the true value of the coefficient of diffusion within micelles and the time between delivery of two diffusion-coded pulse gradients Δ to be identified. The true D_0 and the apparent coefficient of diffusion will coincide whe the mean square displacement of water molecules over time interval Δ is no greater than the micelle radius, or

$$\langle r \rangle \geq \sqrt{6 \cdot \Delta \cdot D_0}. \quad (5)$$

On DW MRI ($b = 0$, 250, 500, 750, and 1000 s/mm^2), in contrast to pure substances, inverse emulsions with mean micelle radius 5 μm show decreases in ADC by 0.02 μm^2/ms when Δ is increased from 44.4 to 60 ms (Table 1).

The accuracy of measurements of ADC using selected samples for different values of the b factor was evaluated by statistical analysis of pixel intensity distributions. It is known that the intensity of signals from the object measured with multichannel RF coils using the sum of squares technique has a non-central χ distribution [14-16]. However, when the signal-to-noise ratio is greater than 5, the non-central χ distribution approximates a Gaussian distribution. The Sturges rule was used to approach separation of grouping into intervals, as this gives the optimum number of intervals [17]. The intensity of the signal from water in the emulsions studied here followed a normal distribution with values of the b factor ranging from 0 to 3000.

TABLE 1. ADC for Different Times Δ

–		Emulsion No. 1	Emulsion No. 2	Emulsion No. 3	Cyclomethicone	Caprylyl	Water
ADC, $\mu m^2/ms$	at Δ = 44.4 ms	0.11	0.09	0.07	0.20	0.30	2.42
	at Δ = 60.0 ms	0.09	0.07	0.05	0.20	0.30	2.42

Thus, the relative deviation of apparent values from the mean *m* for emulsions and pure water was evaluated by calculating the coefficient of variation:

$$V = \frac{\sigma}{m} 100 \ \%, \qquad (6)$$

where σ is the mean square deviation.

For emulsions, this parameter is of the order of 2-4%. A high signal was obtained from emulsions over the whole range of values of *b* studied (from 0 to 10,000 s/mm^2); furthermore, the signal from emulsions established the upper limit for the range of signal intensities at a *b* factor value of greater than 150 s/mm^2 (Fig. 3).

These studies led to development of a phantom (Fig. 4) containing vials of inverse emulsions for assessment not only of the main image quality parameters – signal-to-noise ratio, spatial resolution, etc. – but also for assessment of the accuracy of measurement of ADC on

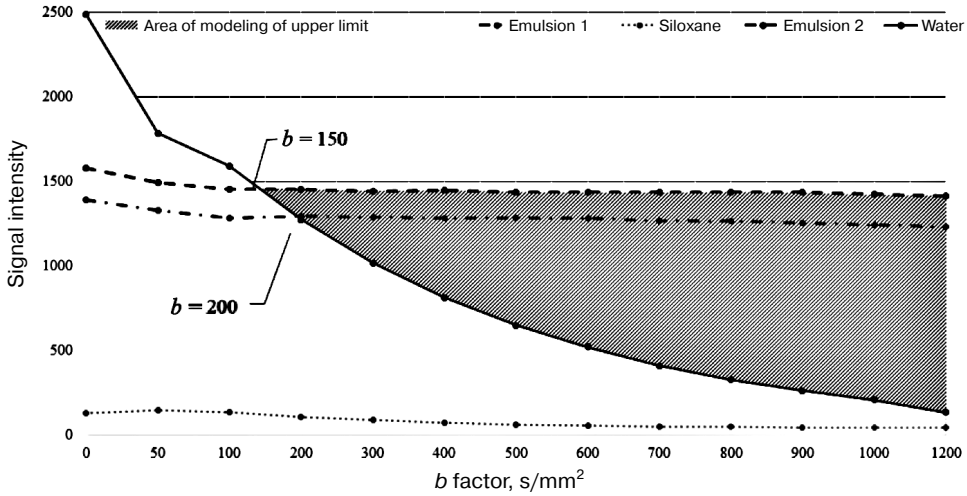

Fig. 3. Relationship between signal intensity and the *b* factor.

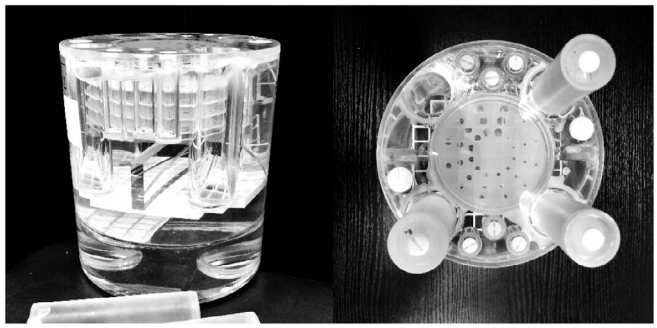

Fig. 4. External view of MRI phantom.

DW MRI images, including when the fat suppression function is used.

Conclusions

This article presents a new method for assessing and standardizing quantitative data on DW images using a phantom containing inverse emulsions based on silicone oils. The monitoring means used here involves assessment of the accuracy of ADC measurement, detection of systematic errors, and cross-calibration of MRI scanners. The micellar model provides for assessment not only of the coefficient of self-diffusion, but also restricted diffusion, in a single measurement. The proposed technical solution is in good agreement with the biexponential model, taking into account the size of tumor cells. The resulting emulsions allow generation of high-intensity signals over a wide range of values of the *b* factor all the way to 10,000 s/mm^2, with low values of ADC modeling malignant formations.

REFERENCES

1. Morozov, A. K., Makhson, A. N., and Karpov, I. N., "Whole-body magnetic resonance tomography (DWIBS). Potentials and perspectives for use in bone pathology," Vestn. Travmatol. Ortop. Imeni N. N. Priorova, No. 2, 19-24 (2015).
2. Bickel, H., Pinker-Domenig, K., Bogner, W., et al., "Quantitative apparent diffusion coefficient as a noninvasive imaging biomarker for the differentiation of invasive breast cancer and ductal carcinoma in situ," Invest. Radiol., **50**, No. 2, 95-100 (2015).
3. Gawande, R. S., Gonzalez, G., Messing, S., et al., "Role of diffusion-weighted imaging in differentiating benign and malignant pediatric abdominal tumors," Pediatr. Radiol., **43**, No. 7, 836-845 (2013).
4. Kivrak, A. S. et al., "Comparison of apparent diffusion coefficient values among different MRI platforms: A multicenter phantom study," Diagnostic Interv. Radiol., **19**, No. 6, 433-437 (2013).
5. Sergunova, K. A., Karpov, I. N., Gromov, A. I., et al., "Development of programmable systems for monitoring quality indicators for diffusion-weighted images to increase the effectiveness of the diagnosis of tumor formations," Biotekhnosfera, **47**, No. 5, 9-13 (2016).
6. Blinov, N. N. and Snopova, K. A., "Problems in the passporting and quality control of magnetic resonance tomography systems," Med. Tekh., **285**, No. 3, 34-37 (2014).
7. Zelikman, M. I., Kruchinin, S. A., and Snopova, K. A., "A method and means of monitoring the operating parameters of magnetic resonance tomographs," Med. Tekh., **263**, No. 5, 27-31 (2010).
8. Choi, M. H., Jeong, S., Nam, S. I., et al., "Rheology of decamethylceclopentalsiloxane (cyclomethicone) W/O emulsion system," Macromol. Res., **17**, No. 12, 943-949 (2009).
9. Skirda, V. D., Maklakov, A. I., Pimenov, G. G., Fatkullin, N. F., Sevryugin, V. A., Dvoyashkin, N. K., Filippov, A. V., and Vasil'ev, G. I., "Development of gradient NMR in studies of the structure and dynamics of complex molecular systems," Str. Dinam. Mol. Sist. (online journal), No. 2 (2018).
10. Guiu, B. and Cercueil, J. P., "Liver diffusion-weighted MR imaging: The tower of Babel?" Eur. Radiol., **21**, No. 3, 463-467 (2011).
11. Li, H., Jiang, X., Xie, J., McIntyre, J. O., et al., "Time-dependent influence of cell membrane permeability on MR diffusion measurements," Magn. Reson. Med., **75**, No. 5, 1927-1934 (2016).
12. Hope, T. R., White, N. S., Kuperman, J., et al., "Demonstration of non-Gaussian restricted diffusion in tumor cells using diffusion time-dependent diffusion-weighted magnetic resonance imaging contrast," Front. Oncol., **6**, Article 179 (2016).
13. Bongers, A., Hau, E., and Shen, H., "Short diffusion time diffusion-weighted imaging with oscillating gradient preparation as an early magnetic resonance imaging biomarker for radiation therapy response monitoring in glioblastoma: A preclinical feasibility study," Int. J. Radiat. Oncol. Biol. Phys. (online journal) (2018), https://www.researchgate.net/publication/322246773_Short_diffusion_time_DWI_with_oscillating_gradient_preparation_as_an_early_MRI_biomarker_for_radiation_therapy_response_monitoring_in_glioblastoma_A_pre-clinical_feasibility_study (accessed: September 21, 2018)
14. Constantinides, C. D., Atalar, E., and McVeigh, E. R., "Signal-to-noise measurements in magnitude images from NMR phased arrays," Magn. Reson. Med., **38**, No. 5, 852-857 (1997).
15. Aja-Fernández, S. and Tristán-Vega, A., "A review on statistical noise models for magnetic resonance imaging," Technical Report of the LPI [online resource], https://www.lpi.tel.uva.es/~santi/personal/docus/noise.survey.tec.report.pdf (accessed: September 19, 2018).
16. Dietrich, O. et al., "Influence of multichannel combination, parallel imaging and other reconstruction techniques on MRI noise characteristics," Magn. Reson. Imaging, **26**, No. 6, 754-762 (2008).
17. Glagolev, M. V. and Sabrekov, A. F., "Recovery of the probability density using a histogram method in soil science and ecology," Dinam. Okruzh. Sred. Global. Izmenen. Klim., No. S1, 55-83 (2008).